Clays and Clay Minerals, Vol. 34, No. 1, 45–52, 1986.

ELECTRON MICROSCOPIC INVESTIGATIONS OF IRON OXYHYDROXIDES AND ACCOMPANYING PHASES IN LATERITIC IRON-CRUST PISOLITES

M. AMOURIC,[1] A. BARONNET,[1] D. NAHON,[2] AND P. DIDIER[2]

[1] Centre de Recherche sur les Mécanismes de la Croissance Cristalline
C.N.R.S.—Campus Luminy, case 913, 13288 Marseille Cédex 9, France

[2] U.A. 721, C.N.R.S., Laboratoire de Pétrologie de la Surface, Université de Poitiers
40, avenue du Recteur Pineau, 86022 Poitiers Cédex, France

Abstract—Pisolites from an iron crust in western Senegal were studied by conventional and high-resolution electron microscopy to determine their internal structure and the genetic processes that led to their formation. Each pisolite consisted of a concentric structure of hematite rimmed by goethite. Two types of goethite were distinguished: (1) large (≃0.6 μm long and 0.06 μm wide), euhedral laths arranged in fibrous aggregates of slightly misoriented grains devoid of internal defects as shown by their two-dimensional lattice images, and (2) a matrix of smaller (≃400 Å), anhedral grains surrounded by the larger laths. Based upon the crystal habit and the presence or absence of internal alveoles, the large goethite laths probably grew at the expense of the matrix goethite. Poorly crystalline kaolinite, presumably formed from well-crystalline precursor kaolinite, and clusters of partially dissolved quartz grains were also imaged. In addition, two uncommon phases were found—maghemite in topotactic relationship with hematite and a layered, Fe-rich, mica-like mineral with a $2M$ superstructure. Unlike kaolinite, this latter phase was likely in equilibrium with iron oxyhydroxides. Substituted Al probably was released during goethite recrystallization, and mass transfers probably took place through the heterogeneous porosity (i.e., large voids and cracks coupled with fine pores) revealed by transmission electron microscopy.

Key Words—Goethite, Hematite, Iron, Kaolinite, Laterite, Lattice fringe image, Pisolite, Transmission electron microscopy.

Résumé—Des pisolites, provenant d'une cuirasse ferrugineuse de l'ouest du Sénégal, ont été étudiés en microscopie électronique conventionnelle et haute résolution dans le but de déterminer leur structure interne et les processus génétiques conduisant à leur formation. Chaque pisolite montre une structure concentrique d'hématite entourée de goethite. Deux types de goethite sont différenciés: (1) des grandes lattes automorphes (≃0,6 μm de long sur 0,06 μm de large) composées de grains légèrement désorientés les uns par rapport aux autres et accolés sous forme de fibres selon $\vec{c}$—ces grains étant dépourvus de défauts internes comme le montrent les images bidimensionnelles de leur réseau, et (2) une matrice de grains plus petits (≃400 Å) et xénomorphes entourés par les grandes lattes. D'après des critères morphologiques et la présence ou l'absence de figures internes de dissolution (pores) il semble que les grandes lattes de goethite se sont développées aux dépens de la matrice de goethite. De la kaolinite mal cristallisée—sans doute dans un état instable—et des agrégats de grains de quartz partiellement dissous sont également imagés. Enfin, deux phases peu communes sont révélées—de la maghemite en relation topotactique avec l'hématite et un minéral en couche type mica, riche en fer et présentant une surstructure $2M$. A l'inverse de la kaolinite, cette dernière phase est vraisemblablement en équilibre avec les oxi-hydroxydes de fer. La substitution de l'aluminium a lieu sans doute durant la recristallisation de la goethite et les transferts de masse se font certainement grâce à l'existence d'une porosité très hétérogène (grands vides, fissures et pores fins) mise en évidence par la microscopie électronique en transmission.

INTRODUCTION

Ferricretes, or hard, iron oxide crusts, are extremely widespread in tropical countries. They result from lateritic weathering of a variety of sedimentary, metamorphic, and igneous rocks (Brückner, 1952) and consist of several superimposed zones, the most evolved of which generally being the highest topographically. Such ferricretes from the Ndias massif of western Senegal, developed on argillaceous sandstone, were described by Nahon (1976, 1985) and Nahon *et al.* (1977). According to these authors, pisolites near the top of this sequence consist of a core rich in Al-hematite surrounded by Al-goethite containing 15–25 mole percent AlOOH. To characterize these pisolites in greater detail and to gain a better understanding of the processes that were responsible for their formation, a conventional and high-resolution electron microscopic study was conducted and is reported in the present paper. The data are also used to comment on the genesis of such well-indurated iron oxide crusts in general.

GENERAL LITHOLOGY

A cross section of the weathering profile of Ndias massif is shown in Figure 1. The Maestrichtian glauconitic sandstone (level h_1) is immediately overlain by a 30-m thick, ochre to red mantle consisting mainly

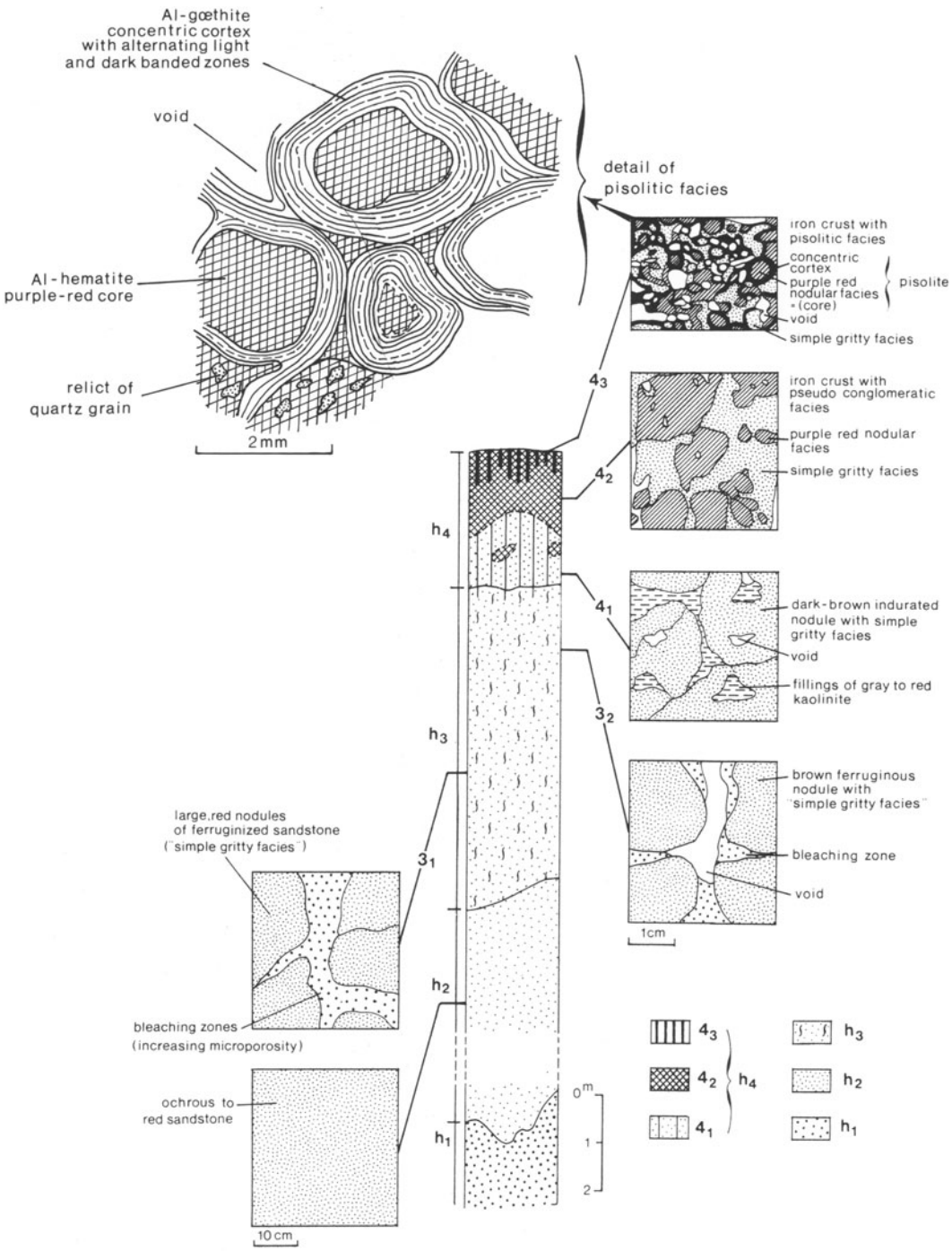

Figure 1. Ferricrete profile of the Ndias massif, western Senegal. h_1 = Maestrichtian glauconitic sandstone; h_2 = weathering mantle, ochre to red sandstone; h_3 = mottled clay horizon with zones of ferruginized gritty facies and bleaching zones (in h_{3_2} voids develop at the expense of bleaching zones); h_4 = iron crust horizon (ferricrete) (in h_{4_1} nodules with gritty facies are dominant, h_{4_2} is iron crust with pseudoconglomeratic facies, h_{4_3} is iron crust with pisolitic facies).

of goethite (2–3%), kaolinite (9–10%), and quartz (about 88%) (level h_2). Level h_3 consists of a more highly ferruginized sandstone containing large iron rich nodules (a few to 20 cm average diameter) in which original quartz grains are cemented by only slightly indurated, crypto- or noncrystalline ferrugineous material. The nodules are immersed in an assemblage of quartz and kaolinite. Paralleling an upward increase in iron con-

https://doi.org/10.1346/CCMN.1986.0340106 Published online by Cambridge University Press

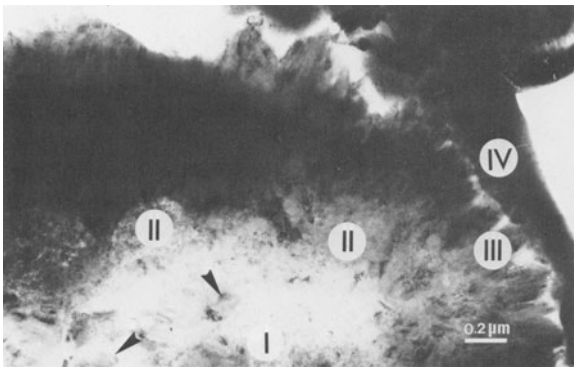

Figure 2. Internal structure of small pisolite. Zone I, fine-grained hematite with some large monocrystals (arrowed); zone II, fine-grained goethite; zone III, large goethite laths; zone IV, quasi-amorphous film.

tent, the mean mineralogical composition of this zone is 80 to 60% quartz, 10 to 40% iron oxyhydroxides, and 10 to 0% kaolinite. Where ferruginization is prevalent, quartz grains are corroded and kaolinite is replaced by goethite + Al-hematite. The Al content of the hematite is about 6–8 mole percent AlOOH, as reported by Nahon *et al.* (1977) and Didier (1983) from X-ray powder diffraction and Mössbauer spectroscopic data, using the method of Janot and Gilbert (1970). Kaolinite and quartz have been leached to the extent of generating voids containing partially dissolved residual quartz grains and booklets of neoformed kaolinite.

The top part of the weathering profile (level h_4) is composed chiefly of layers of pseudoconglomeratic and pisolitic ferricretes. The pseudoconglomeratic horizon consists mainly of purple-red, tightly cemented ferrugineous nodules (1–2 cm average diameter) of Al-hematite (8–15 mole percent Al_2O_3) with relicts of quartz and rare kaolinite. Nodules inherited from level h_3 are also present in this horizon. The uppermost pisolitic horizon was formed by the progressive disappearance of h_3-level nodules. The pisolites of level h_4 contain a network of fine cracks ($\simeq$0.05 mm in size) which show no displacement of the fragments and which are coated with well-crystalline, Al-poor goethite and kaolinite.

EXPERIMENTAL

Uncovered conventional thin sections (30 µm in thickness) were made of iron oxide pisolites. Copper grids were then glued on hematite-rich (core) and goethite-rich (rim) areas of the pisolites as recognized under the optical microscope. The grids were then detached from the thin sections, and the samples were ion-thinned with a dougle-gun ion mill following the procedures outlined by Olives Banos *et al.* (1983) and Amouric and Parron (1985), and finally coated with a thin carbon film. This technique has been found to be well suited for studies of intergranular textures.

A standard Siemens Elmiskop 1A electron microscope (80 kV) was used for low-magnification (TEM), and a Jeol JEM 100C instrument (100 kV) for high-magnification, high-resolution (HRTEM) electron microscopic studies. The latter was equipped with fixed specimen stage and an objective lens with a C_s value of 1.8 mm. Only bright-field images were recorded, using reflections passing through a 40-µm objective aperture. The point-to-point resolution was therefore constrained to >3 Å. Images with optimum defocus (−800 to −1200 Å) were selected from experimental through-focus series.

RESULTS

General texture

Most of the material in the pisolites is hematite or goethite. Figure 2 is a cross section of a pisolite showing a typical texture of four concentric zones. The core consists mainly of a fine-grained structure of hematite crystals (zone I) which is immediately surrounded by fine-grained, goethite-rich mosaic (zone II). Large goethite laths, deeply rooted in zone II form a radiating structure in the external part of the pisolite (zone III). The radiating crystals themselves are coated with a quasi-amorphous film resembling a gel (zone IV).

Iron oxyhydroxides

Hematite. Hematite in the pisolite core occurs as two types of crystals of contrasting grain sizes. Crystals larger than 0.2 µm (Figures 2 and 3) are rare and immersed in a matrix of anhedral crystallites <500 Å in size (Figure 2).

Figure 3 shows a large ion-thinned flake of hematite in the micrometer size range. The crystal is viewed along [0001]. Large bend contours appear mottled in outer regions where Bragg conditions are somewhat relaxed (black arrow in Figure). This aspect is related to dispersed and very fine (40 to 100 Å) intergrowths of a second phase which probably cause a local elastic deformation of the hematite matrix. Also observed in bright-field images are rare stacking fault fringes (white arrow); they are consistent with inclined twin lamellae parallel to $\{10\bar{1}2\}$ or $\{10\bar{1}4\}$ as reported by Bursill and Withers (1979).

The selected area diffraction (SAD) pattern (inset in Figure 3) exhibits the typical (0001) reciprocal net of single-crystal hematite with strong $11\bar{2}0$ (d = 2.51 Å) reflections. In addition, a second hexagonal reciprocal net with strong reflections at d = 2.9–3.0 Å is present. The latter net seems to be radially contracted with respect to the hematite net, and the diffraction spots show some arcing along Debye-Scherrer rings. This type of pattern was found for every hematite crystal examined. Inasmuch as analytical electron microscopy showed only Fe to be present, this second phase must be an iron oxide or oxyhydroxide. Both maghemite

https://doi.org/10.1346/CCMN.1986.0340106 Published online by Cambridge University Press

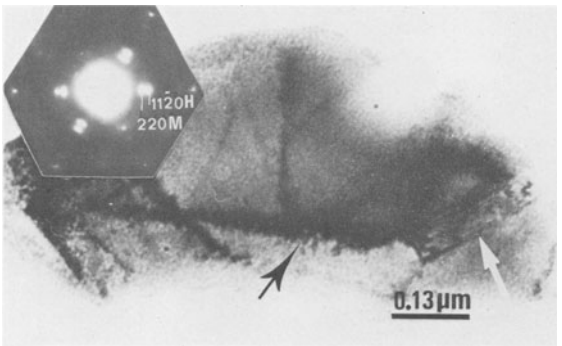

Figure 3. Transmission electron microscopy image of ion-thinned hematite single crystal originally located in core of pisolite. Note speckle contrasts of tiny maghemite "precipitates" (black arrow) and fringe contrast of inclined twin plane (white arrow). Corresponding diffraction pattern (inset).

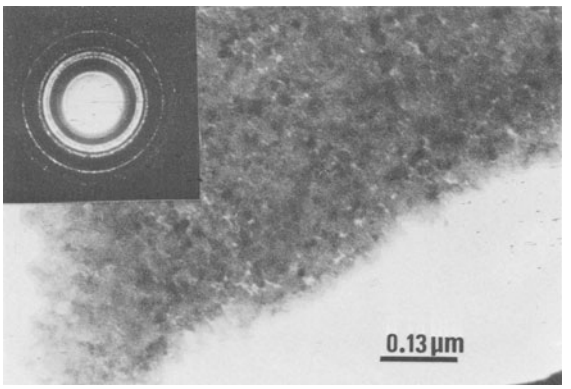

Figure 4. Transmission electron microscopy image showing equigranular texture of goethite from zone II of pisolite and corresponding ring diffraction pattern.

(γ-Fe_2O_3) or magnetite (Fe_3O_4) viewed along ⟨111⟩ could account for such a SAD pattern, wherein the strong 2.9–3.0-Å reflections is indexed as the 220 reflection of maghemite (d(220) = 2.95 Å) or the 220 reflection of magnetite (d(220) = 2.96 Å). From these data, a topotaxic relationship must exist between hematite (α-Fe_2O_3) (H) and maghemite (γ-Fe_2O_3) (1) or magnetite (Fe_3O_4) (2) as follows:

$$(0001)\ (H) \parallel \{111\}\ (1) \text{ or } \{111\}\ (2) \text{ and,}$$
$$\langle 1120\rangle\ (H) \parallel \langle 110\rangle\ (1) \text{ or } \langle 110\rangle\ (2).$$

This topotaxy involves a large ($\simeq$17.5%) misfit ratio between the interface structures of the two phases. The arcing phenomena may be related to azimuthal departures from the exact orientation of many particles with respect to the hematite matrix. No intensity change was noticed for the 220 reflection (1 or 2) during beam exposure indicating that the maghemite or magnetite was not a radiation artifact. Hematite from the fine-grained matrix was imaged by 3.6-Å and 4.5-Å lattice spacings as previously reported by Jefferson *et al.* (1975) and Bursill and Withers (1979). These particles commonly showed a mottled contrast indicative of some destabilization of the structure.

Goethite. The goethite texture found in zone II of the pisolites (see Figure 2) is shown at low magnification in Figure 4. These crystals form compact aggregates of equant and randomly oriented particles 0.05 to 0.1 μm in size. A small but intrinsic intergranular porosity, however, is visible as marked by white sinuous contrasts between grains.

Goethite in zone III occurs as laths elongated along their z-axes with irregular and asymetrically terminated heads (Figure 2) corresponding to a fibrous, intracrystalline texture. Similar habits were reported by Dixon *et al.* (1983). Cross sections of goethite laths normal to the z-axis were examined by HRTEM. Figures 5a, 5b, and 5c show cross sections cut through the boundary between zones II and III. Figure 5a is a two-dimensional lattice image of goethite viewed along the z-axis in which (010) lattice fringes with a spacing of ~10 Å are modulated as dots along [100] with a ~4.6-Å periodicity. A perfect one-to-one correspondence between image and the goethite structure is reached in the encircled part of Figure 5a. Here, additional white spots are visible between the bright (010) spot rows such that all white spots match the empty tunnels between rows of octahedra seen on end in the goethite structure. From Figures 5a and 5b, it is clear that the grains are anhedral and rounded except in the upper right part of Figure 5a where the trace of a {110} face can be observed. Furthermore, these crystals are divided into subgrains, such as those marked A and B, all having their z-axis in common. The subgrains are perfect with regard to lattice defects, and the subgrain boundaries are more (Figure 5b) or less (Figure 5a) open. These subgrains are probably cross sections of the component fibers forming goethite laths. Internal cracks parallel to the ⟨110⟩ directions (Figure 5b) were noted as well as rhombic alveoles (Figure 5c) outlined by ⟨110⟩ directions. These alveoles are similar to HCl-etch features recently reported by Schwertmann (1984) on synthetic goethite. Such cracks and alveoles strongly suggest that the goethite from the boundary between zones II and III experienced late dissolution after growth.

Goethite crystals protruding into voids or cracks between pisolite fragments (*vide supra*) are characterized by an euhedral habit of component fibers ({110} rhombic cross sections) as seen in Figure 5d. Neither dissolution cracks nor alveoles were observed, indicating a phase that was not exposed to late dissolution.

Silicates

Several silicate phases coexisting with hematite and goethite in the pisolites were also imaged with HRTEM. Among them, kaolinite was found mainly with he-

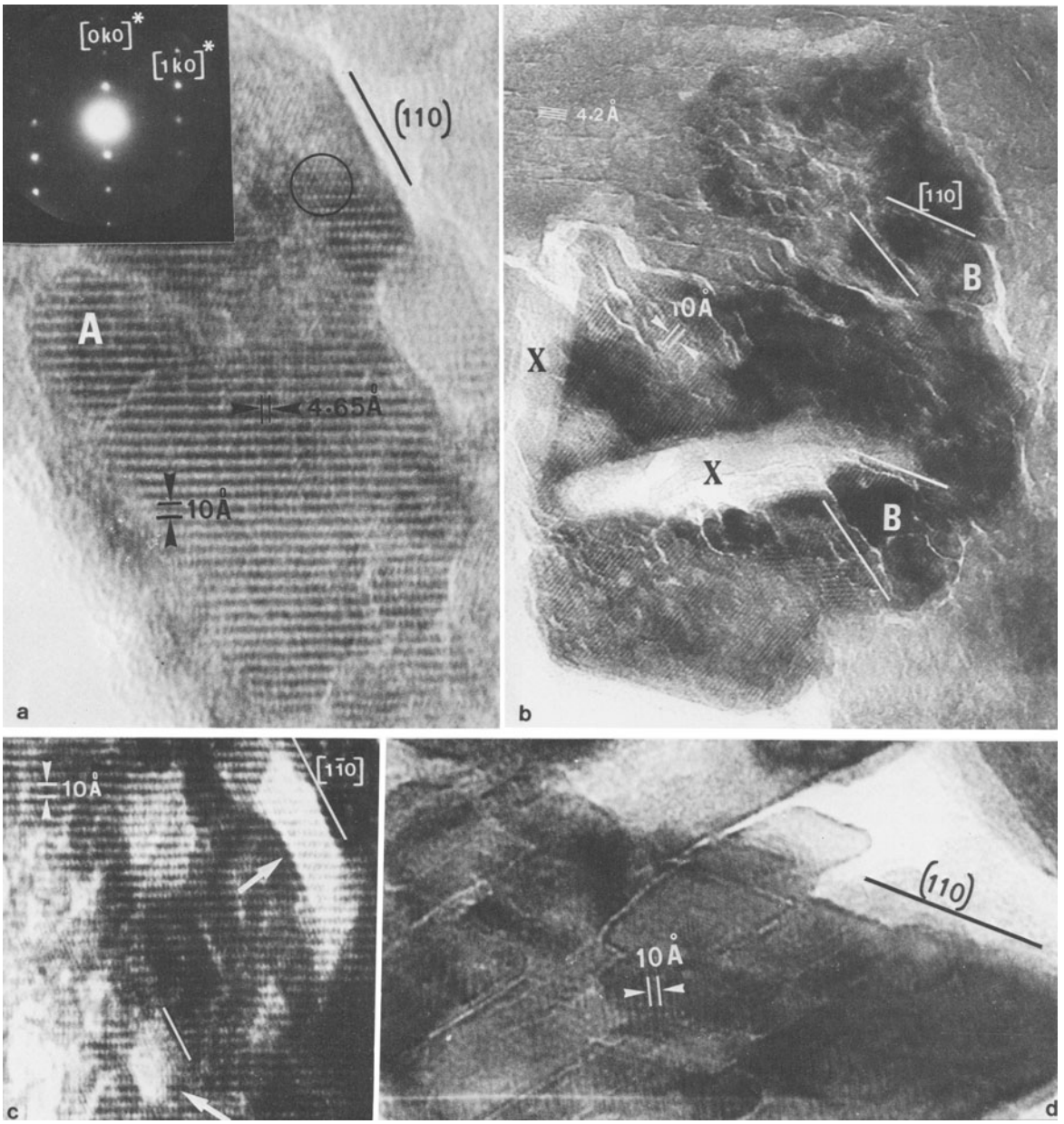

Figure 5. Lattice fringe images of goethite from zone III. (a) Two-dimensional image of crystal viewed along [001] or [00$\bar{1}$]. Circled part displays most detailed structure image for this mineral. Subgrain (A) is slightly shifted with respect to crystal matrix. Note rounded outline of this section except for {110} trace in upper right. Corresponding diffraction pattern in inset. (b) Rounded cross section of lath exhibiting specific 10-Å (010) lattice fringe system and longitudinal section with 4.2-Å (110) lattice fringes, on left. (B) domains are slightly rotated around *c* with respect to mineral matrix. Two lighter lath-shaped zones (X) correspond to another phase completely removed by ion-thinning. (c) Two-dimensional image of crystal viewed along [001] or [00$\bar{1}$]. Rhombic alveoles (arrowed), with edges parallel to ⟨110⟩, indicate dissolution. (d) Almost perfect rhombic section of fresh lath protruding into voids between pisolite fragments. Note composite aspect of this as-grown goethite and its perfect ⟨110⟩ morphology.

matite (region I). A rather poorly organized sheet structure was revealed by blurred, locally interrupted and wavy lattice fringe contrasts (Figure 6). These peculiar symptoms indicate a poor crystallinity for kaolinites in tropical laterites (Herbillon *et al.*, 1976; Mestdagh *et al.*, 1982), and probably correspond to a partial decomposition of this mineral.

Clusters of equant quartz grains (Figure 7) were also found in the hematite-rich (I) and goethite-rich (II + III) zones. These grains are almost defect-free except

https://doi.org/10.1346/CCMN.1986.0340106 Published online by Cambridge University Press

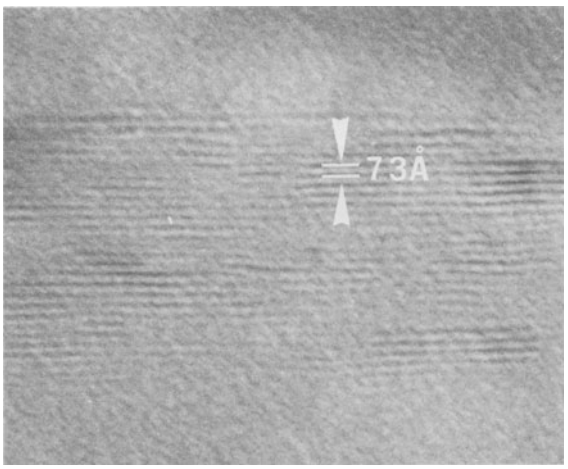

Figure 6. Typical (001) lattice fringes of kaolinite lath which denote rather poorly organized structure.

for occasional subgrain boundaries marked by dislocation walls. Triple and quadruple junctions of grain boundaries produce voids which are outlined by triangles or rectangles. The voids are probably indicative of a pervasive dissolution of quartz grains. Chemical exchanges with the outside may have taken place through these dissolution voids.

Commonly grouped as packets in the goethite matrix of zone III are platelets of a layered mineral (Figure 8a). Qualitative microanalyses of such platelets (Figure 8b) revealed chiefly Fe with minor Si and Al and locally traces of P, but no alkali elements. The HRTEM lattice image in Figure 9 shows a regular 10.2-Å basal spacing. Moreover, when two-dimensional lattice images could be recorded on this electron-beam sensitive phase (Figure 10), a two-layer superstructure (2*M* polytype) was

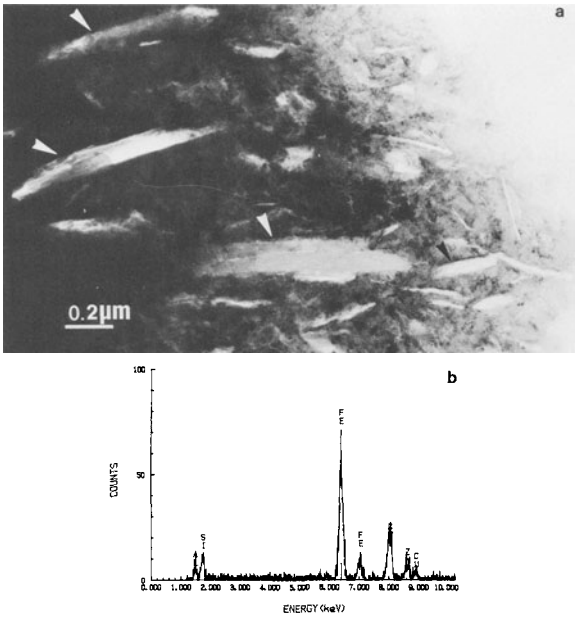

Figure 8. (a) Concentration of platelets of a layered mineral in zone III, as shown by arrow heads. (b) Qualitative microchemical analysis of such platelets (Cu and Zn are due to specimen stage).

identified. Both chemical and structural data suggest a mica-like, Fe-rich, alkali-poor phyllosilicate. This material is similar to a mineral not fully identified by Jefferson *et al.* (1975) in an HRTEM study of kaolinites which were iron-stained by goethite.

DISCUSSION AND CONCLUSION

Two contrasting size ranges were found for both hematite and goethite. Small hematite grains from the pisolitic core were much more numerous than larger

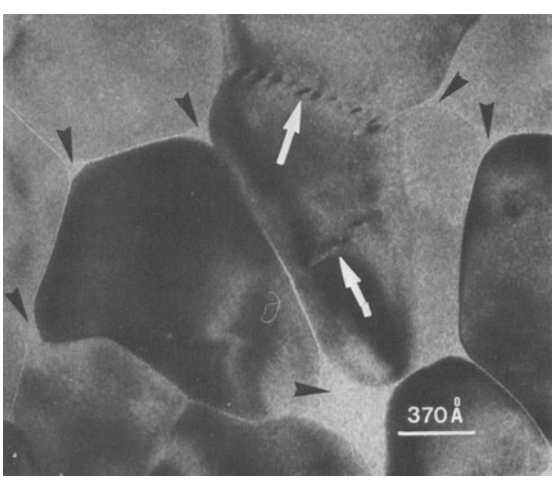

Figure 7. Mosaic of rounded quartz grains in pisolite. Black arrows show fine pores between grains and white arrows indicate dislocation walls between subgrains.

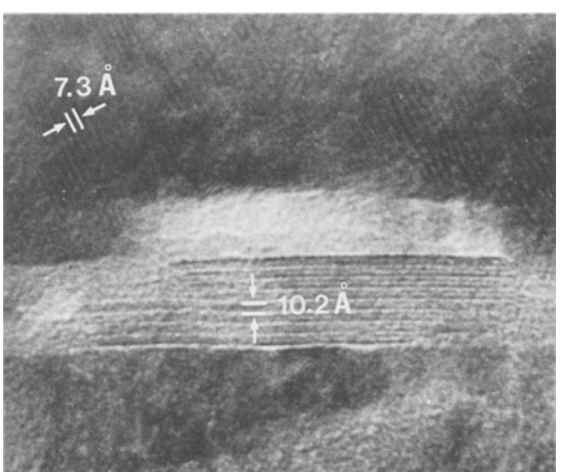

Figure 9. Platelet of well-organized layered mineral showing regular 10.2-Å fringes and large and poorly contrasted kaolinite area (d(001) ≃ 7.3 Å).

https://doi.org/10.1346/CCMN.1986.0340106 Published online by Cambridge University Press

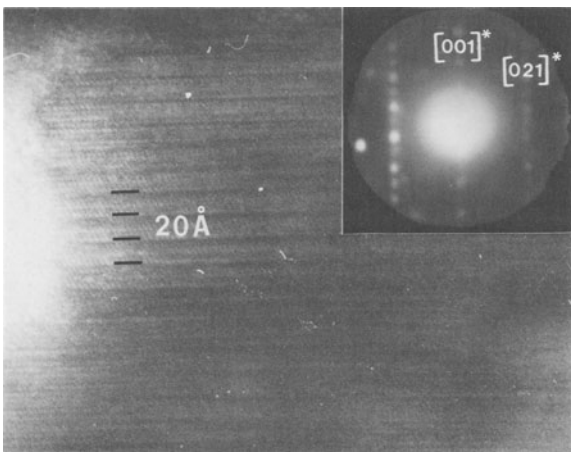

Figure 10. Two-dimensional image of thicker section of sheet structure shown in Figure 9. Black bars underline regular $2M$ stacking sequence of this Fe-phyllosilicate (d(001) ≃ 20 Å). Corresponding diffraction pattern in inset.

flakes in the same location. Their TEM-determined sizes (<450 Å) fall within the 40–400-Å size range previously estimated from Mössbauer spectra (Didier, 1983). Smaller and larger goethite crystals were clearly localized in the matrix of zone II and in zone III of the pisolites, respectively. Mean grain sizes of goethite of such pisolitic material as a whole, as inferred from Mössbauer spectra and X-ray powder diffraction data, were in the range 40 to 150 Å (Didier, 1983), i.e., well below those actually observed by TEM (≃400 Å for equant particles or more for subgrains as coherent domains in goethite composite laths). Inasmuch as neither equant particles nor subgrains contained internal defects, such a discrepancy cannot be explained. A repeatedly negative correlation between the Al/Fe substitution ratio in Fe-oxyhydroxides and kaolinites and the size of the particles has been reported (see Janot and Gilbert, 1970; Torrent *et al.,* 1980; Cases *et al.,* 1982). This relationship has been shown also in the Ndias system (Nahon, 1976; Nahon *et al.,* 1980; Didier, 1983) where the substitution ratio increases and the grain size decreases, towards the top of the lateritic profile. For goethite, equant-size texture likely corresponds to more Al-rich compositions than those of larger lath-shaped crystals; however, further microchemical analyses are needed.

Regarding the topotactic relationship between the iron oxide precipitate and the hematite host, maghemite is probably present because magnetite is not likely to form under the highly oxidizing conditions present in the uppermost part of a weathering profile. The presence of maghemite associated with hematite has previously be pointed out in pisolites from Australian ferricretes (Faniran, 1970) and in other laterites (e.g., Taylor and Schwertmann, 1974).

From the TEM observations of habit, the internal features (vacuoles and cracks), and the crystallinity of component phases of the pisolites, conclusions may be drawn regarding their growth or dissolution behavior. Quartz, kaolinite, and small hematite and goethite grains probably underwent dissolution or destabilization, whereas the protruding parts of goethite laths as well as the Fe-rich phyllosilicate experienced growth only. Thus, due to the radial distribution of such crystals in the pisolite, external crystals probably developed at the expense of internal crystals. Although weathering systems are open, it is likely that Si and Al from quartz + kaolinite were transported over only a few micrometers to form the Si-Al part of the stable mica-like mineral. Part of the Al from kaolinite and the Fe from hematite was first reused to crystallize a first generation of Al-rich goethite, and the remaining Fe was used to complete the Fe-rich phyllosilicate. The latter phase, in equilibrium with oxyhydroxides, was probably stabilized because it was able to accept more Fe^{3+} than kaolinite for which the maximum $Fe_2Si_2O_5(OH)_4$ content does not exceed 3% mole (Mestdagh *et al.,* 1980; Herbillon *et al.,* 1976). Ultimately, the first generation of Al-rich goethite recrystallized at the periphery of a pisolite as Al-poor, lath-shaped goethite.

Inside the pisolite, the required mass transfer of elements probably took place through the intergranular spaces revealed by TEM, whereas materials for the growth of the final goethite were mostly transported through the large voids between pisolites, where noncrystalline matter has been found.

From the bottom to the top of the weathering profile (*vide supra*), kaolinite and quartz decrease whereas iron oxyhydroxides increase. This trend corresponds to a progressive upward ferruginization of the weathered material. In detail, this evolution proceeds by iteration of dissolution and recrystallization of quartz, kaolinite, and oxyhydroxides (Nahon, 1976). These processes are mostly controlled by changes in the environmental conditions prevailing at any time and position in the weathering system, but the role of the accompanying and evolving porosity of the material (Tardy and Nahon, 1985) is also important. Such macroscopic mineralogical trends across the weathering profile are about the same as those revealed by TEM studies inside the pisolites of the iron-crust zone as successive mineral neoformations. These neoformations are merely responses at any time to an evolving chemical system. Therefore, such well-indurated iron-crust zones are not "end-products" of weathering, but rather intermediate products of a still evolving system.

REFERENCES

Amouric, M. and Parron C. (1985) Structure and growth mechanism of glauconite as seen by high-resolution transmission electron microscopy: *Clays & Clay Minerals* **33,** 473–482.

Brückner, W. (1952) The mantle rock ("laterite") of the Gold Coast and its origin: *Geol. Rdsch.* **43,** 307–327.

Bursill, L. A. and Withers, R. L. (1979) On the multiple orientation relationships between hematite and magnetite: *J. Appl. Cryst.* **12,** 287–294.

Cases, J. M., Lietard, U., Yvon, J., and Delon, J. F. (1982) Etude des propriétés cristallochimiques, morphologiques et superficielles de kaolinites désordonnées: *Bull. Minéral.* **105,** 439–455.

Didier, P. (1983) Paragenèses à oxydes et hydroxydes de fer dans les bauxites et les cuirasses ferrugineuses: Thèse 3ème cycle, Université de Poitiers, 150 pp.

Dixon, J. B., Golden, D. C., Calhoun, F. G., and Buseck, P. R. (1983) Synthetic aluminous goethite investigated by HRTEM: in *Proc. 41st Annual Meeting Electron Microscopy Soc. Amer., Phoenix, Arizona,* J. W. Bailey, ed., San Francisco Press, San Francisco, 192–193.

Faniran, A. (1970) Maghemite in the Sydney duricrust: *Amer. Miner.* **55,** 925–933.

Herbillon, A. J., Mestdagh, M. M., Vielvoye, L., and Derouane, E. G. (1976) Iron in kaolinite with special references to kaolinite from tropical soils: *Clay Miner.* **2,** 201–219.

Janot, C. and Gilbert, H. (1970) Les constituants du fer dans certaines bauxites naturelles étudiées par effet Mössbauer: *Bull. Soc. Fr. Minér. Cristall. Paris* **93,** 213–223.

Jefferson, D. A., Tricker, M. J., and Winterbottom, P. A. (1975) Electron microscopic and Mössbauer spectroscopic studies of iron-stained kaolinite minerals: *Clays & Clay Minerals* **23,** 355–360.

Mestdagh, M. M., Herbillon, A. J., Rodrique, L., and Rouxhet, P. G. (1982) Evaluation du rôle du fer structural sur la cristallinité des kaolinites: *Bull. Minéral.* **105,** 457–466.

Mestdagh, M. M., Vielvoye, L., and Herbillon, A. J. (1980) Iron in kaolinite: II. The relationship between kaolinite crystallinity and iron content: *Clay Miner.* **15,** 1–13.

Nahon, D. (1976) Cuirasses ferrugineuses et encroûtements calcaires au Sénégal occidental et en Mauritanie. Systèmes évolutifs: géochimie, structures, relais et coexistence: *Sci. Géol. Mém. Strasbourg* **44,** 1–232.

Nahon, D. (1985) Evolution of ferricretes in tropical landscapes: in *Rates of Chemical Weathering of Rocks and Minerals,* W. Colman, ed., Academic Press, New York (in press).

Nahon, D., Carozzi, A. V., and Parron, C. (1980) Lateritic weathering as a possible mechanism for the generation of ferruginous ooids: *J. Sedim. Petrol.* **50,** 1287–1298.

Nahon, D., Janot, C., Karpoff, A. M., Paquet, H., and Tardy, Y. (1977) Mineralogy, petrography and structures of iron crust (ferricretes) developed on sandstones in the Western part of Senegal: *Geoderma* **19,** 263–277.

Olives Banos, J., Amouric, M., De Fouquet, C., and Baronnet, A. (1983) Interlayering and interlayer slip in biotite as seen by HRTEM: *Amer. Mineral.* **68,** 754–758.

Schwertmann, U. (1984) The influence of aluminium on iron oxides: IX. Dissolution of Al-goethites in 6 M HCl: *Clay Miner.* **19,** 9–19.

Tardy, Y. and Nahon, D. (1985) Stability of Al-goethite, Al-hematite and Fe^{3+}-kaolinite in bauxites, ferricretes and laterites. An approach of the mechanism of the concretion formation. *Amer. J. Sci.* (in press).

Taylor, R. M. and Schwertmann, U. (1974) Maghemite in soils and its origin: I. Properties and observations of soil maghemite: *Clay Miner.* **10,** 299–310.

Torrent, J., Schwertmann, U., and Schulze, D. G. (1980) Iron oxide mineralogy of some soils of two river terrace sequences in Spain: *Geoderma* **23,** 191–208.

(Received 20 October 1984; accepted 20 May 1985; Ms. 1418)